Supplementary Material for Quantitative Evaluation of Base and Detail Decomposition Filters Based on their Artifacts

Charles Hessel and Jean-Michel Morel

We present here some supplementary material, organized as follow:

- Section I and Section II present material on the related works that we believe helps to seize the context of our evaluation.
- We provide in Section III some important information on the complexity of the filters we discarded from our study.
- Section IV allows to better appreciate the objective evaluation of filters thanks to visual inspection of filtered patterns.
- Section V displays results with natural images.

I. Related work on quality assessment studies

A. Perceptual quality assessment

In their 2002 report [1] and 2003 short paper [2], Drago *et al.* evaluated seven tone-mapping methods, with a group of eleven participants. They did "pairwise comparisons of images that led to an ordering of the images according to which were more or less natural looking". Their objective was to find the attribute most predictive of the success of TMOs. They found that the apparent level of detail was first and the naturalness second. They identified an "ideal" point in a *stimulus space* obtained from the analysis of their subjective measures. Its location suggests that "the best tone mapping operator should produce images balanced in detail reproduction and contrast reduction". The authors observed that "higher contrast images were not preferred nor regarded as more natural; rather, a moderate contrast coupled with higher detail (. . .) was most preferred". More importantly, they report that "several unacceptable artifacts were identified, including improper reproduction of overall brightness, totally cropped luminance around light sources, and loss of detail in the images darker regions".

Yoshida *et al.* [3] pursued this work in a psychological study where fourteen human observers evaluated seven TMOs by comparing the tone-mapped images against the real scenes. They wanted to find out which attributes are taken into account by the participants. The human subjects rated image naturalness, overall contrast, overall brightness, and detail reproduction in dark and bright image regions. The authors concluded that "none of the image appearance attributes has a strong influence on the perception of naturalness by itself", and proposed that "this may suggest that naturalness is dependent on a combination of the other attributes".

Ledda *et al.* [4] carried out psychophysical experiments on six tone mapping operators using pair-wise comparisons with linearly mapped HDR scenes displayed on a HDR screen. The experiments involved a large number of people (109) and scenes (23). They carried out two independent studies on the overall similarity and detail reproduction, respectively. They also investigated the influence of color in the perceived quality of the operators with an experiment using grayscale images and concluded that color has no significant impact on the overall ranking of the TMOs.

In [5], Čadík *et al.* evaluated the overall quality of tone-mapped images with subjective psychological tests. They provided a ranking of the tone-mapping operators and analyzed the dependencies of the subjective overall image quality assessment on four selected basic image attributes: *brightness*, *contrast*, *color* and *detail*. They considered 14 tone-mapping operators and conducted two subjective perceptual studies based on two groups of 10 non-experts subjects. In the first experiment, the human observer was asked to *rate* the tone-mapping operators with reference to a real (indoor) scene, both for the overall image quality and the four attributes. In the second experiment, the real scene was not available to the subject, who was asked to *rank* printouts of the same 14 tone-mapped images for the overall image quality and the four attributes. The author found that a simple linear regression was good enough to explain the overall quality (*OIQ*) in function of the four attributes, with the following weights:

$$OIQ_{2006} = 0.327\ brightness + 0.267\ contrast + 0.230\ color + 0.102\ detail.$$

Čadík *et al.* completed this evaluation in 2008 [6], where they made two notable additions. First, they used two additional real (outdoor) scenes. Then, they considered several *artifacts* as additional basic attributes. They identified:

- *halo artifacts*, which correspond to our luminance halo,
- *color artifacts*, coming from superficial handling of colors and leading to poor color preservation of over-saturation,
- *quantization artifacts*, which stem from a strong enhancement of values encoded with low precision. This is similar to the staircase effect, but with a different cause.

Charles Hessel and Jean-Michel Morel are with CMLA, ENS Cachan, CNRS, Université Paris-Saclay, 94235 Cachan, France

The updated linear model of the *overall image quality* they obtained is

$$OIQ_{2008} = 0.07\ \textit{brightness} + 0.37\ \textit{contrast} + 0.06\ \textit{detail} + 0.36\ \textit{color} + 0.21\ \textit{artifacts},$$

meaning that the *artifacts* measure has a strong influence on the perceived overall quality of the tone-mapped image.

Kuang *et al.* conducted in 2007 [7] a perceptual evaluation of tone-mapping operators. This followed previous psychological experiments in 2004 [8] and 2005 [9] where 30 observers were asked to choose the preferred tone-mapped image in pairs. In their 2007 paper, the authors realized three experiments. First, a "paired-comparison" for the overall image preference. Then a "rating-scale" experiment where they analyzed the correlation between image attributes and the overall preference. These two first experiments were carried out with 12 scenes using an LDR display, whereas in the third one the tone-mapped images were evaluated with reference to three actual (physical) scenes. Experiment 1 included 33 participants in the first part (color tone-mapping) and 23 in the second part (gray-scale tone-mapping); experiments 2 and 3 included 19 participants. They compared 6 TMOs, considering 6 basic image attributes: *contrast* in the *highlights*, *contrast* in the *shadows*, *colorfulness* in the *highlights*, *colorfulness* in the *shadows*, *overall contrast*, and *overall accuracy*. One of the conclusions of this series of studies was that the preference evaluation has a strong positive correlation with the accuracy evaluation, which would mean that the most pleasant images are also the most accurate in terms of rendering. Also, they obtain that "gray-scale tone-mapping performance correlates very well with the overall preference".

In a consecutive work in 2010, Kuang *et al.* [10] used an HDR display to evaluate 7 TMOs on 4 scenes, with 23 participants. They found from their two experiments (one using real-world scene comparison, the other using an HDR screen) that the "visual assessments obtained from the HDR display and those obtained from real-world scenes are in good agreement". Like in the 2007 paper, their best ranked TMOs have a local component.

Akyüz *et al.* [11] in 2007 made perceptual studies on the process of *inverse* tone-mapping. Their problem was to evaluate the different ways to display an LDR image on a HDR screen. An interesting outcome of this study is that "HDR images that are tone-mapped for display on standard monitors are often no better than the best single LDR exposure from a bracketed sequence", and that "simply boosting the range of an LDR image linearly to fit the HDR display can equal or even surpass the appearance of a true HDR image". One of the experiments consisted in asking the participants to *rank* six images. The authors used unusual higher-level attributes: *naturalness*, *visual appeal*, *spaciousness* and *visibility*.

In 2013, Eilertsen *et al.* [12] evaluated eleven tone-mapping operators intended for video. Two experiments were made. In the first one, they asked 5 experts to judge the TMOs according to 7 attributes, "selected to capture the most common problems": the overall *brightness*, overall *contrast*, overall *color saturation*, temporal color *consistency*, *flickering*, *ghosting* and *noise*. It is notable that the three before-last attributes are *artifacts* due to the temporal dimension of video. Similarly to our methodology, the first experiment described by the authors is the identification of artifacts by a group of five experts. They were indeed asked to recognize the problems of the different TMOs; and these qualitative evaluation was summarized in a table which gives for each TMO and each attribute a degree of "acceptability" among three: "critical problems that to a large extent affect the perceived visual quality of the tone reproduction; issues of less obvious character, but which add to a weaker outcome of the operator; no visible artifacts or weaknesses". From this first evaluation seven TMOs were short-listed for the second experiment, where 18 participants evaluated 5 tone-mapped sequences using pair-wise comparisons. They did not intend to rank the operators, but they were able to tell the three TMOs that performed the best on the considered clips. An interesting point from the point of view of our paper is the way the parameters were set by involving four experts. The authors extended their work in 2017 with objective measures [13]. This is described in Section I-B.

A deeper survey of TMO evaluation studies can be found in [14] and [15]. Both note the difficulty to carry out such measures and the great variability of the results. For example in the presented studies, some concluded that the *local* TMOs were preferred over the *global* ones [4], [7], [10], while some other studies reached the exact contrary conclusion [5], [6], [11]. These differences can have different origins, for example the experimental setup, evaluation criteria used, the way the experiment is explained to the subject, and so forth. This is well described by Eilertsen *et al.* in [14], where the authors also make this interesting observation concerning the strong variability of ranking between the global and local operators: "The quality may also be masked by spatial inconsistencies, or artifacts, which are more common when a local tone compression is applied". This observation is important. We observed that when the quality of the tone-mapped (or contrast-enhanced) image is evaluated by image experts, artifacts take a particularly high importance and lead to veto images that might be appealing for the rest. The notion of artifact is also largely present in the review of the visual quality assessment in [15].

All the above-presented papers use basic attributes such as brightness, contrast and color. In order to avoid the difficulties of perceptual evaluation, numerous propositions were made to create objective measures of these attributes. They are reviewed in the next section. Most studies acknowledge the presence of artifacts, which has even been considered as a basic attribute [6], [12]. Yet no attempt has been made to measure them objectively. This, we believe, is due to a quite vague definition of *what is an artifact*.

B. *Quantative direct measures of basic image attributes*

Given the difficulty of subjective evaluations, several attempts to automatically measure the quality of tone-mapped images have been proposed. Quite similarly to the subjective evaluations, one can categorize them in 1) full-reference quality measures, where the original image (reference) is used and 2) reference-free quality measures, where it is not. These methods try to evaluate the aesthetic quality of images using some statistical tests.

1) Full-reference quality metrics: Aydin *et al.* in 2008 [16] proposed a metric for the comparison of images with different dynamic ranges. This method is based on the *visible distortions* from the point of view of the human visual system, and has been validated with perceptual experiments. The authors considered three cases of contrast modification: loss of visible contrast; amplification of invisible contrast and reversal of visible contrast. The "visible" or "invisible" thresholds are obtained using a model of human vision. The output of their detector is a probability map for each of those criteria. Note that the contrast reversal measurement is quite related to the *staircasing artifact* we consider in this paper.

Inspired by the success of the structural similarity index (SSIM) method for image quality assessment, Yeganeh *et al.* [17] proposed in 2010 an objective assessment algorithm that creates multi-scale similarity maps between HDR and LDR images. In 2013, they added another criterion to their objective measurement called the statistical naturalness [18]. So their 2013 metric consist of two scores:

- *Structural Fidelity* (S), based on a modified structural similarity index;
- *Statistical Naturalness* (N) , based on intensity statistics of natural images;

from which they derive a meta score called *Overall quality* (Q) which integrates the structural fidelity, and the statistical naturalness

$$Q = aS^{\alpha} + (1-a)N^{\beta}, \tag{1}$$

where $a = 0.8012$, $\alpha = 0.3046$ and $\beta = 0.7088$. These scores are obtained by regression using subjective data. Note that the score N is in fact reference-free.

In their 2017 paper, Eilertsen *et al.* [13] carried out an extensive review of tone-mapping algorithms for HDR videos. They provide in this paper a "quantitative assessment on a set of video tone-mapping algorithms, where [they] formulate a measure to compare them in terms of a number of important properties". The properties they consider are *temporal coherence*, *contrast*, *noise visibility* and *exposure*. Rather than generating a single quality score, they intended to evaluate the operators in terms of the different attributes. In the **temporal coherence** measure, they compare the tone-mapped sequence to the HDR input using the cross-correlation but modified so as to be invariant to local linear changes in time. This way the measure is sensitive to flickering but not to adaptation over time. The **contrast** measure is obtained using the detail layer computed with the bilateral filter. This is combined with a more global measure of the contrast using the mean of the local standard-deviation. The **noise visibility** is measured using the HDR-VDP-2 quality predictor [19] proposed by Mantiuk *et al.* in 2011, using a reference noise-free computer-generated image. Finally, the **exposure** is measured as the number of pixels either above 0.95 or under 0.02.

2) Reference-free quality metrics: Aydin *et al.* [20] proposed in 2015 five reference-free metrics: *sharpness*, *depth*, *clarity*, *tone* and *colorfulness*. Their goal was to rate image aesthetic attributes rather than detecting distortions, so this work is out of our focus. Interestingly enough though, many of their metrics involve the decomposition of the input image in base and detail (they use the domain transform).

Some other methods implicitly use reference-free quality measures. For example, the Exposure Fusion paper [21], [22] uses measures of *color*, *contrast* and *well-exposedness* that aim at characterizing the quality of pixels in an image. They can directly serve as reference-free image quality assessment measures.

Work on video quality assessment can be found in Aydin *et al.* [23] and Yeganeh *et al.* [24]. For a more complete and general review of the quality assessment method we refer to [15], [25]–[27].

II. Description of filters

A. A few more filters, discarded for their complexity

For a sake of completeness we mention a few other interesting enhancement filters and explain why we discarded them in our comparison. The low curvature image simplifier filter (LCIS) proposed in 1999 by Tumblin and Turk [28] can decompose an image in a base and detail layers well adapted to contrast manipulation. Their filter is related to the anisotropic diffusion. The solution of their partial differential equation tends to regions with uniform gradients (low curvature), instead of constant regions in AD. Hence, their filter produces a piece-wise affine approximation of the input image rather than a piece-wise constant one. Unfortunately, the solution of this equation is a slow iterative process that makes it unpractical for large images. Moreover, the tone-mapping operator they propose involves several applications of LCIS. To give an order of magnitude, Fattal *et al.* [29] indicates 8.5 minutes for a 751×1130 pixels image. Moreover, the coefficients in LCIS must be adapted to each image [30], which does not correspond to our need of an automatic decomposition. For these many reasons we omit LCIS in our comparison. It can anyway be represented by the iterated guided filter, since they belong to the same family of anisotropic diffusion related iterated filters.

In 2009, Subr *et al.* [31] proposed an edge-preserving filter in which they define the detail as the oscillations between local extrema. They first find the extrema locations, then construct two envelopes using an edge-aware diffusion technique proposed by Levin *et al.* [32]. The base layer is then obtained as the mean between the maximal and minimal envelopes. This filter has three drawbacks from our point of view: first, the produced detail has very high amplitude oscillations, which are not appropriate to tone-mapping or contrast enhancement. Second, it causes a strong compartmentalization effect. Furthermore, the complexity of this filter is rather high, making it unpractical for large neighborhood and large images.

B. Enhancement filters that do not decompose images in base and detail

Several classic filters perform direct enhancement of the image without base and detail decomposition. Some perform local processing prone to creating artifacts. They are nonetheless outside the scope of our artifact measurements, as the detail layer is not available. We shall nonetheless include them in our visual comparison in the final Section V. The filters we shall consider are: multi-scale retinex (MSR), automatic color enhancement (ACE), histogram equalization (HE) and contrast-limited adaptive histogram equalization (CLAHE). They are the most representative filters of this family. Some other tone-mapping operators are available in the literature, which we chose to omit in this comparison. We explain our decision below.

In 2002, Fattal *et al.* [29] published a “gradient domain high dynamic range compression” technique. This method directly computes the output image by defining its gradients in function of the input image’s one. More precisely, it computes the gradients and applies a spatially-varying compressing function that reduces the amplitude of large edges and preserves the amplitude of small ones. That is, $G(x, y) = \nabla I(x, y)\Phi(x, y)$, where G are the gradients of the output image, $\nabla I(x, y)$ those of the input image and Φ the compressing function. Because the 2D gradient field G is not necessarily integrable, they approximate the solution by seeking the minimum of $\int \|\nabla I(\mathbf{x}) - G\|^2 d\mathbf{x}$, where $\mathbf{x} = (x, y)$. This least squares problem leads to solving a large system of equations. In order to perform base and detail decomposition one can modify Φ so that the large edges are preserved and the small ones smoothed out. This algorithm actually already exists, it is WLS and is part of the final contest.

Ward Larson *et al.* [33] in 1997 proposed a global histogram adjustment method, efficient when the input histogram has empty portions, but limited when the input exhibits a uniform histogram. In 1998, Pattanaik *et al.* [34] presented a tone-mapping operator based upon psychophysically-derived filter banks. This technique has the drawback of presenting luminance halos. Other global tone-mapping operators can be found in *e.g.* Reinhard *et al.* [35] and Drago *et al.* [36]. A third option is to perform both global and local manipulation, as proposed in the two-stage algorithm by Ferradans *et al.* [37], later extended by Cyriac *et al.* in [38]. These methods are based upon neural and psychophysical models of visual perception. In the same spirit, Benzi *et al.* [39] recently used the virtual retina simulator [40], developed by Wohrer *et al.* in 2009 in neuroscience to model the retina (it transforms a video into spike trains) to build a tone-mapping operator for videos. We refer to the Reinhard *et al.* book [25] that gives a good review of a number of tone-mapping operators until 2010.

III. Filters complexity

We now compare the computational times of all methods. Rapidity is required, because the decomposition in base + detail is only a part of complex image pipelines, and generally positioned ahead of other treatments. All filters have a main parameter controlling the amount of detail extracted by the method, or, put another way, the amplitude of what is considered as detail. This parameter greatly changes the final result of enhancement chains, so it is generally left to the user for fine-tuning. This, however, requires displaying a preview of the final result in real-time. Giving a ranking of the filters in function of their execution time is difficult, as it is highly dependent both on the implementation and the machine used for the tests. We can nonetheless base our ranking on the theoretical complexities. These are summarized in Table I.

The guided filter have a linear complexity with respect to the image size N. The fast local Laplacian filter FLL have basically the same complexity as its single-scale version, that is, the same complexity as FBF. Indeed it simply involve $\frac{4}{3}N$ pixels instead of N. This number is the total number of pixels in a Gaussian/Laplacian pyramid. The fast approximation of the bilateral filter using the Paris-Durand approach (FBF and FLL) have a dependence on R, the dynamic range of the image. But they downsample the volume NR in function of σ_s and σ_r, so the higher these parameters, the faster the filter. The domain transform is one of the fastest filters available for edge-aware smoothing; it has an $\mathcal{O}(N)$ complexity with a slope smaller than the GF and FBF in function of the dimensionality.

IV. Tables of results with the patterns

The Table II, Table III, Table IV, Table V are displayed all the filtered versions of the patterns for the luminance halo, the staircase effect, the compartmentalization and the contrast halo, respectively.

V. Application to natural images

We present the decomposition results of the seven considered filters for five natural images in a series of three tables. The first displays the base layers, see Table VI. The following displays the detail layers. See Table VII. These tables may be the more appropriate to compare the results because the details better highlight differences between filters. The third table presents enhanced images. See Table VIII. The enhancement algorithm is very simple and does not involve a final stretching (we use clipping instead) so as to provide comparable results. The displayed images are computed using

$$\textit{enhance}(u) = .125 + .750 \times \sqrt{\mathrm{EAF}\{u\}} + 3 \times (u - \mathrm{EAF}\{u\}), \tag{2}$$

where EAF stands for any edge-aware filter. In short, we apply a square-root to the base layer (which is the simplest classic gamma-correction) and slightly shrink its dynamics, while the detail layer is amplified. We suppose the input dynamic range in $[0, 1]$.

The blurry image with the obelisk (fourth column) is particularly relevant for the staircase effect. One can easily distinguish the inverted contrast band along the obelisk for the bilateral-based filters (apart from the multi-scale bilateral filter

[1] In Le Guen *et al.* paper [41] at page 209, one sees that each iteration has roughly 15 operations per pixel (op/pix) and that the recommended iteration number is about 200 (page 210). This amounts to a complexity of 3000 op/pix. As this decomposition is rather local, the number of iterations is arguably independent from the image size, for a given scale parameter.

[2] Strange horizontal oscillations with amplitude 1 appear in TV-L^1 results. This is due to the conversion from double to unsigned 8bits integer needed in their implementation. This is not due to the algorithm itself, and have extremely little influence on the measures.

[3] See Footnote 2.

Table I
SUMMARY OF THE CONSIDERED FILTERS' COMPLEXITY (AND ABBREVIATIONS).

Abbr.	Method	Complexity
DT	Domain Transform (recursive filter)	$\mathcal{O}(N)$
IS-L^0	L^0 image smoothing	$\mathcal{O}(N \log N)$
FBF	Fast bilateral filter (bilateral grid) ($R \Leftrightarrow$ dynamic range)	$\mathcal{O}(N + \frac{N}{\sigma_s^2}\frac{R}{\sigma_r})$
FLL	Fast local Laplacian filter	$\mathcal{O}(N + \frac{R}{\sigma_r})$
GF	Guided filter	$\mathcal{O}(N)$
TV-L^1	Total variation using L^1 norm	$\mathcal{O}(3000N)$[1]
WLS	Weighted least squares	$\mathcal{O}(N)$

Table II
LUMINANCE HALO MEASUREMENT. THE DYNAMIC RANGE OF ALL RESULTS IS $[-0.04, +0.04]$.[2]

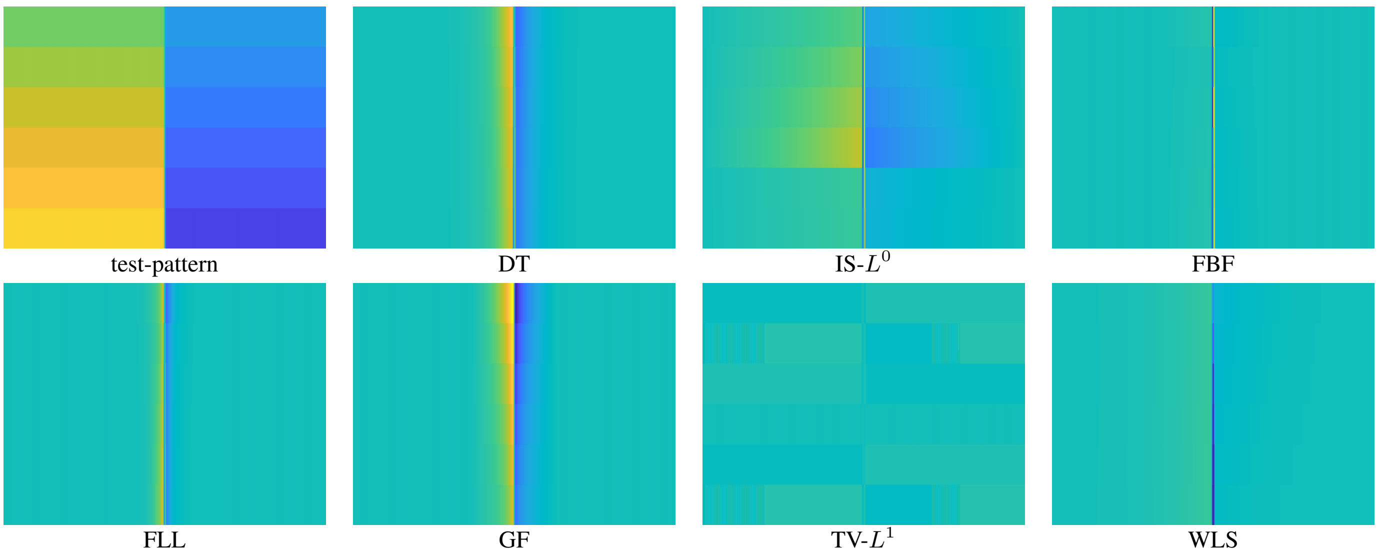

Table III
STAIRCASE EFFECT MEASUREMENT. THE DYNAMIC RANGE OF ALL RESULTS IS $[-0.03, +0.03]$. THE STAIRCASING APPEARS AS BLUE LINES ON THE LEFT PART OF THE TEST-PATTERN AND A YELLOW LINE ON THE RIGHT PART. ON THE CONTRARY, YELLOW ON THE LEFT AND BLUE ON THE RIGHT REVEAL LUMINANCE HALO BUT THIS EFFECT CAN BE BETTER APPRECIATED IN TABLE II.[3]

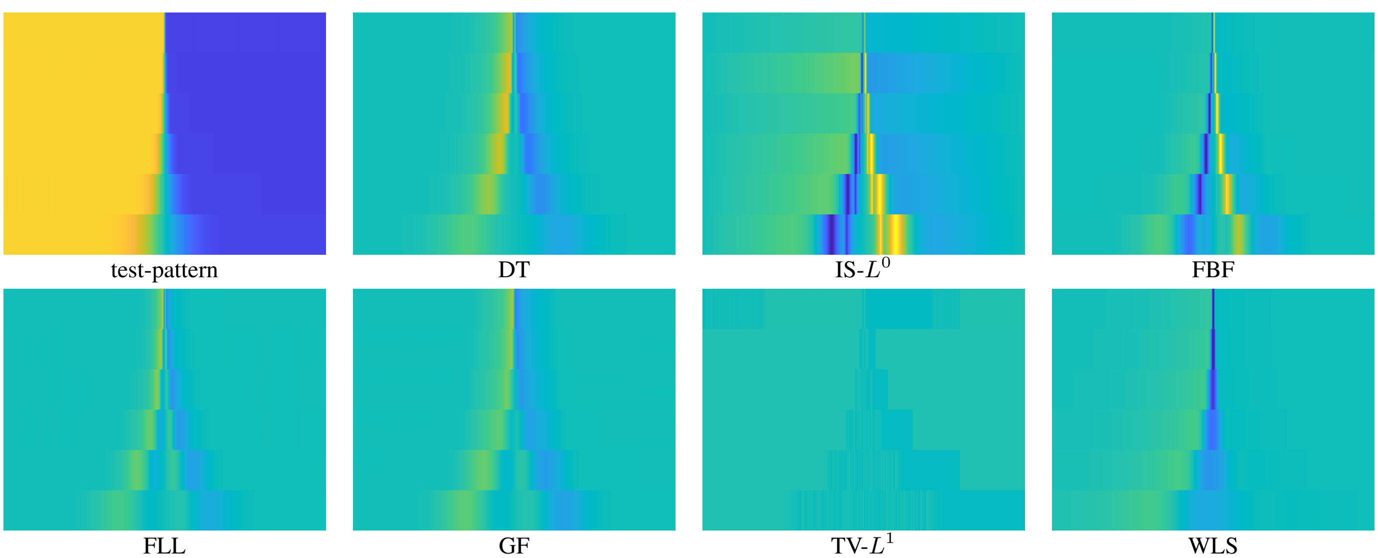

Table IV
COMPARTMENTALIZATION EFFECT MEASURE. THE DISPLAYED DYNAMIC IS $[-0.1, +0.1]$. THE MORE YELLOW SQUARES AND DARK BLUE LINES, THE MORE COMPARTMENTALIZATION.

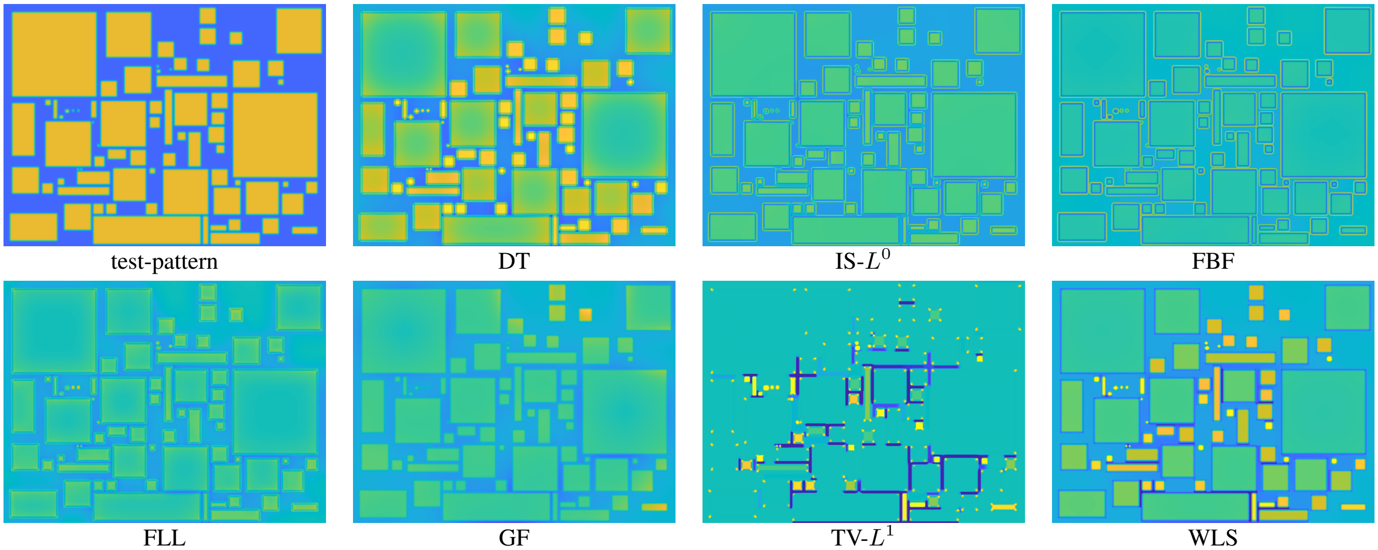

Table V
CONTRAST HALO MEASUREMENT. THE DISPLAYED DYNAMIC RANGE IS $[-0.1, +.01]$. THE LESS TEXTURE IS EXTRACTED ALONG THE LINES AND COLUMNS, THE STRONGER THE CONTRAST HALO.

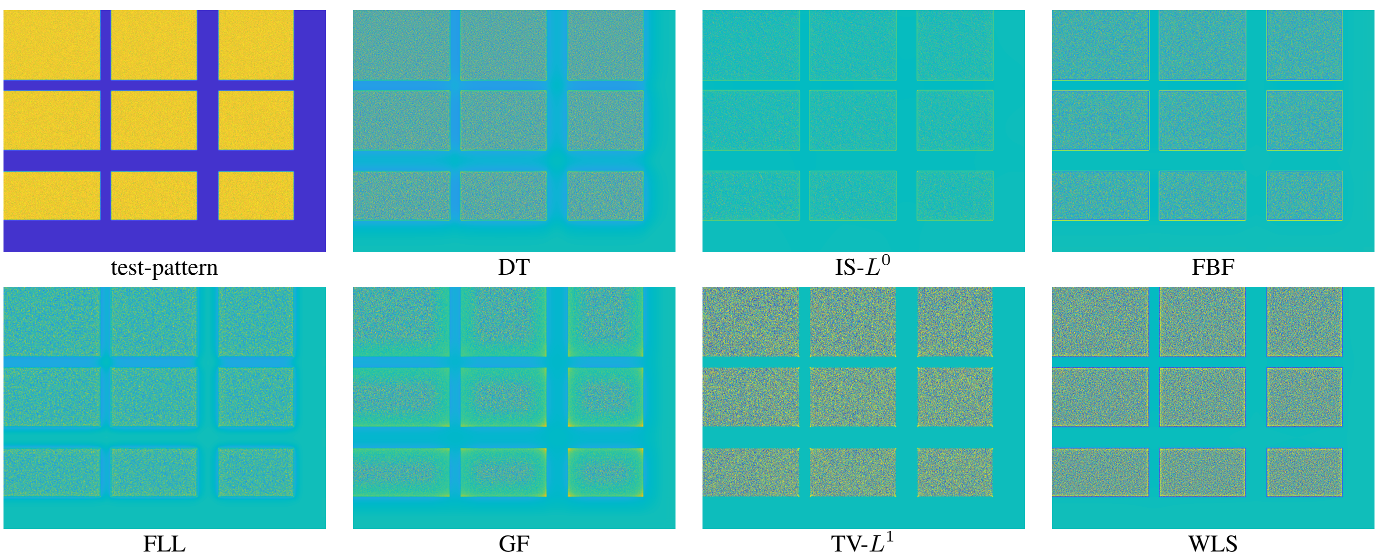

with regression), IS-L^0 and the iterated guided filter. The trellis image (third column) is particularly relevant for the contrast halo artifact, as well as the first image with the hat. The hat is also good at showing the luminance halo, at the transition between the hat and the ceiling. The image in the second row can help see the luminance halo around the streetlight and in the clouds. The compartmentalization artifact is visible between the branches in the picture of the fifth column.

REFERENCES

[1] F. Drago, W. L. Martens, K. Myszkowski, and H.-P. Seidel, "Perceptual evaluation of tone mapping operators with regard to similarity and preference," Max Planck Institut Fur Informatik, Stuhlsatzenhausweg 85, 66123 Saarbrücken, Germany, Tech. Rep. 2, 2002. 1

[2] ——, "Perceptual evaluation of tone mapping operators," in *ACM SIGGRAPH 2003 Sketches & Applications*. ACM, 2003, pp. 1–1. 1

[3] A. Yoshida, V. Blanz, K. Myszkowski, and H.-P. Seidel, "Perceptual evaluation of tone mapping operators with real-world scenes," in *Procedings of SPIE, Human Vision and Electronic Imaging X*, B. E. Rogowitz, T. N. Pappas, and S. J. Daly, Eds., vol. 5666, mar 2005, p. 192. [Online]. Available: http://proceedings.spiedigitallibrary.org/proceeding.aspx?doi=10.1117/12.587782 1

[4] P. Ledda, A. Chalmers, T. Troscianko, and H. Seetzen, "Evaluation of tone mapping operators using a High Dynamic Range display," *ACM Transactions on Graphics*, vol. 24, no. 3, p. 640, jul 2005. [Online]. Available: http://portal.acm.org/citation.cfm?doid=1073204.1073242 1, 2

[5] M. Čadík, M. Wimmer, L. Neumann, and A. Artusi, "Image attributes and quality for evaluation of tone mapping operators," in *Proceedings of the 14th Pacific Conference on Computer Graphics and Applications*. Taipei, Taiwan: National Taiwan University Press, 2006, pp. 35– 44. 1, 2

Table VI
NATURAL IMAGES, BASE LAYERS

Table VII
NATURAL IMAGE, DETAIL LAYERS (CENTERED AROUND 127.5 AND MULTIPLIED BY A FACTOR 3 FOR VISUALIZATION).

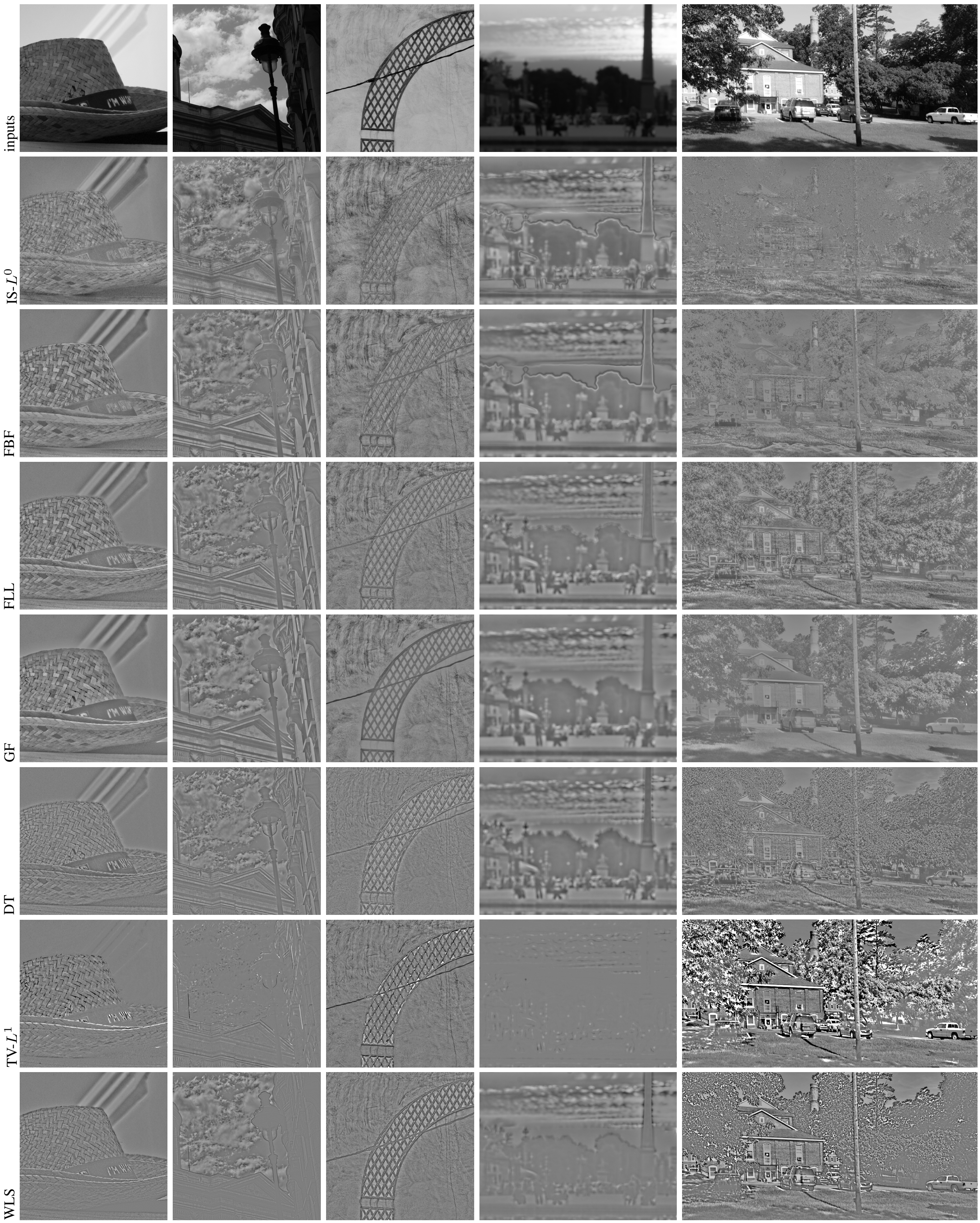

Table VIII
NATURAL IMAGES, ENHANCED IMAGES USING $\textit{enhance}(u) = .125 + .750 \times \sqrt{\mathrm{EAF}\{u\}} + 3 \times (u - \mathrm{EAF}\{u\})$.

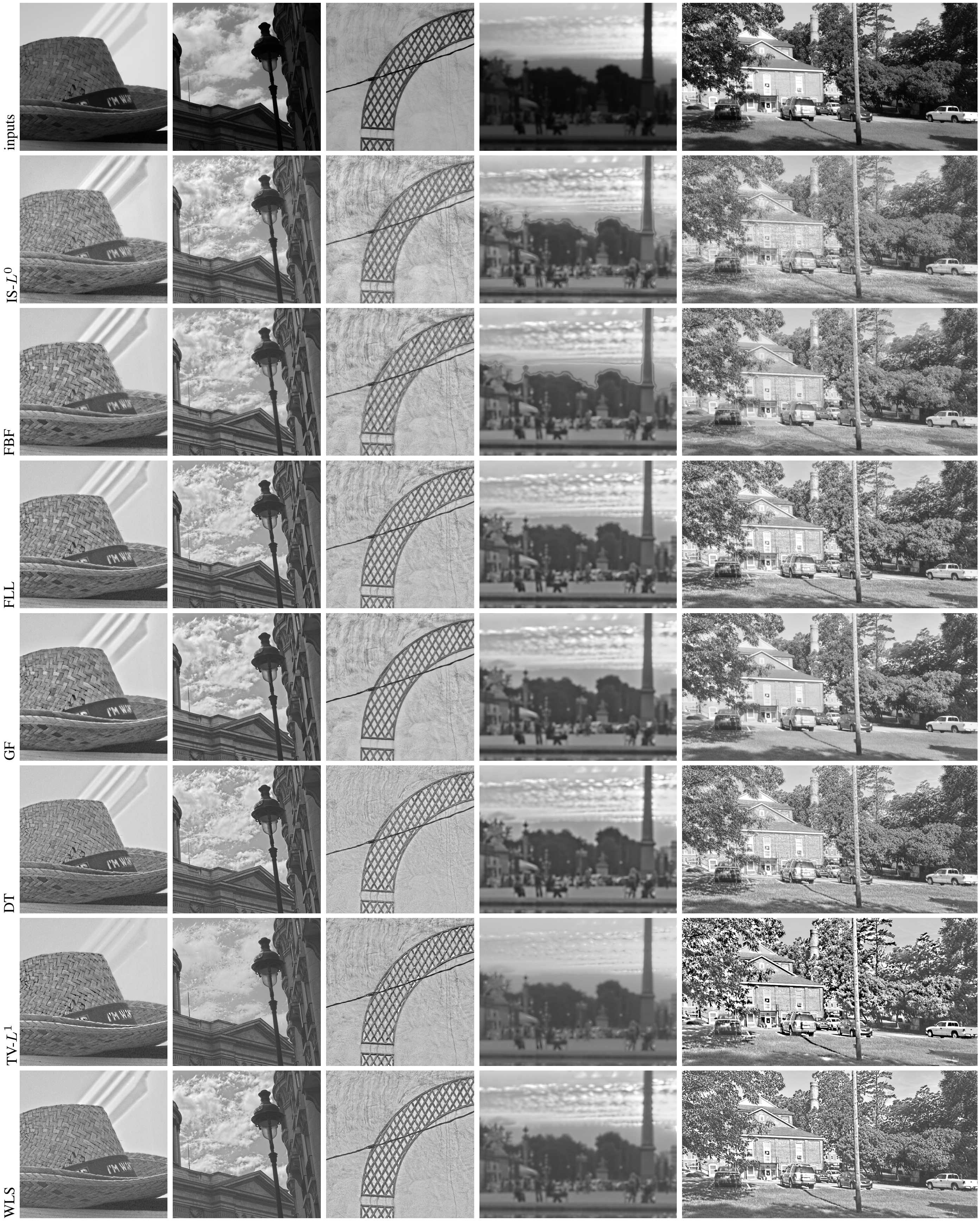

[6] M. Čadík, M. Wimmer, L. Neumann, and A. Artusi, "Evaluation of hdr tone mapping methods using essential perceptual attributes," *Computers & Graphics*, vol. 32, no. 3, pp. 330 – 349, 2008. [Online]. Available: http://www.sciencedirect.com/science/article/pii/S0097849308000460 1, 2

[7] J. Kuang, H. Yamaguchi, C. Liu, G. M. Johnson, and M. D. Fairchild, "Evaluating HDR rendering algorithms," *ACM Transactions on Applied Perception*, vol. 4, no. 2, pp. 9–es, jul 2007. [Online]. Available: http://portal.acm.org/citation.cfm?doid=1265957.1265958 2

[8] J. Kuang, H. Yamaguchi, G. M. Johnson, and M. D. Fairchild, "Testing hdr image rendering algorithms," in *Color and Imaging Conference*, vol. 2004, no. 1. Society for Imaging Science and Technology, 2004, pp. 315–320. 2

[9] J. Kuang, G. M. Johnson, and M. D. Fairchild, "Image preference scaling for hdr image rendering," in *Color and Imaging Conference*, vol. 2005, no. 1. Society for Imaging Science and Technology, 2005, pp. 8–13. 2

[10] J. Kuang, R. Heckaman, and M. D. Fairchild, "Evaluation of HDR tone-mapping algorithms using a high-dynamic-range display to emulate real scenes," *Journal of the Society for Information Display*, vol. 18, no. 7, p. 461, 2010. [Online]. Available: http://doi.wiley.com/10.1889/1.1828693 2

[11] A. O. Akyüz, R. Fleming, B. E. Riecke, E. Reinhard, and H. H. Bülthoff, "Do HDR displays support LDR content?" *ACM Transactions on Graphics*, vol. 26, no. 3, p. 38, jul 2007. [Online]. Available: http://portal.acm.org/citation.cfm?doid=1276377.1276425 2

[12] G. Eilertsen, R. Wanat, R. K. Mantiuk, and J. Unger, "Evaluation of Tone Mapping Operators for HDR-Video," *Computer Graphics Forum*, vol. 32, no. 7, pp. 275–284, oct 2013. [Online]. Available: http://doi.wiley.com/10.1111/cgf.12235 2

[13] G. Eilertsen, R. K. Mantiuk, and J. Unger, "A comparative review of tone-mapping algorithms for high dynamic range video," *Computer Graphics Forum*, vol. 36, no. 2, pp. 565–592, may 2017. [Online]. Available: http://doi.wiley.com/10.1111/cgf.13148 2, 3

[14] G. Eilertsen, J. Unger, and R. K. Mantiuk, "Evaluation of tone mapping operators for hdr video," in *High Dynamic Range Video*. Elsevier, 2016, pp. 185–207. 2

[15] G. Lavoué and R. Mantiuk, "Quality Assessment in Computer Graphics," in *Visual Signal Quality Assessment*. Cham: Springer International Publishing, 2015, pp. 243–286. [Online]. Available: http://link.springer.com/10.1007/978-3-319-10368-6{_}9 2, 3

[16] T. O. Aydin, R. Mantiuk, K. Myszkowski, and H.-P. Seidel, "Dynamic range independent image quality assessment," *ACM Trans. Graph.*, vol. 27, pp. 69:1–69:10, Aug. 2008. [Online]. Available: http://doi.acm.org/10.1145/1360612.1360668 3

[17] H. Yeganeh and Z. Wang, "Objective assessment of tone mapping algorithms," in *2010 IEEE International Conference on Image Processing*. IEEE, sep 2010, pp. 2477–2480. [Online]. Available: http://ieeexplore.ieee.org/document/5651778/ 3

[18] ——, "Objective quality assessment of tone-mapped images," *IEEE Transactions on Image Processing*, vol. 22, no. 2, pp. 657–667, 2013. [Online]. Available: https://ece.uwaterloo.ca/{~}z70wang/publications/TIP{_}TMQI.pdf 3

[19] R. Mantiuk, K. J. Kim, A. G. Rempel, and W. Heidrich, "HDR-VDP-2: A calibrated visual metric for visibility and quality predictions in all luminance conditions," in *ACM SIGGRAPH 2011 papers on - SIGGRAPH '11*, vol. 1, no. 212. New York, New York, USA: ACM Press, 2011, p. 1. [Online]. Available: http://portal.acm.org/citation.cfm?doid=1964921.1964935 3

[20] T. O. Aydin, A. Smolic, and M. Gross, "Automated aesthetic analysis of photographic images," *IEEE Transactions on Visualization and Computer Graphics*, vol. 21, no. 1, pp. 31–42, 2015. [Online]. Available: https://pdfs.semanticscholar.org/3396/f8eb0439d780d173c108cca7ba01e69f0cbc.pdf 3

[21] T. Mertens, J. Kautz, and F. Van Reeth, "Exposure fusion," in *Computer Graphics and Applications, 2007. PG '07. 15th Pacific Conference on*, Oct 2007, pp. 382–390. 3

[22] ——, "Exposure fusion: A simple and practical alternative to high dynamic range photography," *Computer Graphics Forum*, vol. 28, no. 1, pp. 161–171, 2009. [Online]. Available: http://dx.doi.org/10.1111/j.1467-8659.2008.01171.x 3

[23] T. O. Aydin, M. Čadík, K. Myszkowski, and H.-P. Seidel, "Video quality assessment for computer graphics applications," *ACM Transactions on Graphics*, vol. 29, no. 6, p. 1, dec 2010. [Online]. Available: http://portal.acm.org/citation.cfm?doid=1882261.1866187 3

[24] H. Yeganeh, S. Wang, K. Zeng, M. Eisapour, and Z. Wang, "Objective quality assessment of tone-mapped videos," in *2016 IEEE International Conference on Image Processing (ICIP)*, vol. 2016-Augus. IEEE, sep 2016, pp. 899–903. [Online]. Available: http://ieeexplore.ieee.org/document/7532487/ 3

[25] E. Reinhard, W. Heidrich, P. Debevec, S. Pattanaik, G. Ward, and K. Myszkowski, *High dynamic range imaging: acquisition, display, and image-based lighting*. Morgan Kaufmann, 2010. 3, 4

[26] Z. Wang and A. C. Bovik, *Modern Image Quality Assessment*. Morgan & Claypool, jan 2006, vol. 2, no. 1. 3

[27] W. Lin and C. C. Jay Kuo, "Perceptual visual quality metrics: A survey," *Journal of Visual Communication and Image Representation*, vol. 22, no. 4, pp. 297–312, may 2011. [Online]. Available: http://linkinghub.elsevier.com/retrieve/pii/S1047320311000204 3

[28] J. Tumblin and G. Turk, "A Boundary Hierarchy For Detail-Preserving Contrast Reduction," in *Proceedings of the 26th annual conference on Computer graphics and interactive techniques - SIGGRAPH '99*. New York, New York, USA: ACM Press, 1999, pp. 83–90. [Online]. Available: http://portal.acm.org/citation.cfm?doid=311535.311544 3

[29] R. Fattal, D. Lischinski, and M. Werman, "Gradient domain high dynamic range compression," *Proceedings of the 29th annual conference on Computer graphics and interactive techniques - SIGGRAPH '02*, vol. 21, no. July 2002, p. 249, 2002. [Online]. Available: http://portal.acm.org/citation.cfm?doid=566570.566573 3, 4

[30] F. Durand and J. Dorsey, "Fast bilateral filtering for the display of high-dynamic-range images," *ACM Trans. Graph.*, vol. 21, pp. 257–266, Jul. 2002. [Online]. Available: http://doi.acm.org/10.1145/566654.566574 3

[31] K. Subr, C. Soler, and F. Durand, "Edge-preserving multiscale image decomposition based on local extrema," *ACM Transactions on Graphics*, vol. 28, no. 5, p. 1, dec 2009. [Online]. Available: http://portal.acm.org/citation.cfm?doid=1618452.1618493 3

[32] A. Levin, D. Lischinski, and Y. Weiss, "Colorization using optimization," *ACM Transactions on Graphics*, vol. 23, no. 3, p. 689, aug 2004. [Online]. Available: http://portal.acm.org/citation.cfm?doid=1186562.1015780http://portal.acm.org/citation.cfm?doid=1015706.1015780 3

[33] G. Larson, H. Rushmeier, and C. Piatko, "A visibility matching tone reproduction operator for high dynamic range scenes," *IEEE Transactions on Visualization and Computer Graphics*, vol. 3, no. 4, pp. 291–306, 1997. [Online]. Available: http://ieeexplore.ieee.org/document/646233/ 4

[34] S. N. Pattanaik, J. A. Ferwerda, M. D. Fairchild, and D. P. Greenberg, "A multiscale model of adaptation and spatial vision for realistic image display," in *Proceedings of the 25th annual conference on Computer graphics and interactive techniques - SIGGRAPH '98*. New York, New York, USA: ACM Press, 1998, pp. 287–298. [Online]. Available: http://portal.acm.org/citation.cfm?doid=280814.280922 4

[35] E. Reinhard, M. Stark, P. Shirley, and J. Ferwerda, "Photographic tone reproduction for digital images," *ACM Transactions on Graphics*, vol. 21, no. 3, pp. 267–276, 2002. [Online]. Available: http://portal.acm.org/citation.cfm?doid=566654.566575 4

[36] F. Drago, K. Myszkowski, T. Annen, and N. Chiba, "Adaptive Logarithmic Mapping For Displaying High Contrast Scenes," *Computer Graphics Forum*, vol. 22, no. 3, pp. 419–426, sep 2003. [Online]. Available: http://doi.wiley.com/10.1111/1467-8659.00689 4

[37] S. Ferradans, M. Bertalmio, E. Provenzi, and V. Caselles, "An analysis of visual adaptation and contrast perception for tone mapping," *IEEE Transactions on Pattern Analysis and Machine Intelligence*, vol. 33, no. 10, pp. 2002–2012, Oct 2011. 4

[38] P. Cyriac, M. Bertalmío, D. Kane, and J. Vazquez-Corral, "A tone mapping operator based on neural and psychophysical models of visual perception," in *Human Vision and Electronic Imaging XX*, vol. 9394. International Society for Optics and Photonics, 2015, pp. 9394 – 9394 – 10. [Online]. Available: https://doi.org/10.1117/12.2081212 4

[39] M. Benzi, M.-J. Escobar, and P. Kornprobst, "A bio-inspired synergistic virtual retina model for tone mapping," *Computer Vision and Image Understanding*, vol. 168, no. November 2017, pp. 21–36, mar 2018. [Online]. Available: https://doi.org/10.1016/j.cviu.2017.11.013http://linkinghub.elsevier.com/retrieve/pii/S1077314217302047 4

[40] A. Wohrer and P. Kornprobst, "Virtual Retina: A biological retina model and simulator, with contrast gain control," *Journal of Computational Neuroscience*, vol. 26, no. 2, pp. 219–249, apr 2009. [Online]. Available: http://link.springer.com/10.1007/s10827-008-0108-4 4

[41] V. L. Guen, "Cartoon+ Texture Image Decomposition by the TV-L1 Model," *Image Processing On Line*, vol. 4, pp. 204–219, 2014. [Online]. Available: http://www.ipol.im/pub/art/2014/103/ 4